Science of the Total Environment 639 (2018) 1394–1407

Contents lists available at ScienceDirect

Science of the Total Environment

journal homepage: www.elsevier.com/locate/scitotenv

Integrated assessments of green infrastructure for flood mitigation to support robust decision-making for sponge city construction in an urbanized watershed

Chao Mei [a], Jiahong Liu [a,b,*], Hao Wang [a,b], Zhiyong Yang [a], Xiangyi Ding [a], Weiwei Shao [a]

[a] China Institute of Water Resources and Hydropower Research, State Key Laboratory of Simulation and Regulation of Water Cycle in River Basin, China, Beijing 100038, China
[b] School of Transportation and Civil Engineering & Architecture, Foshan University, Guangdong 528000, China

HIGHLIGHTS

- Hydrological responses of GI implementation investigated under six rainfall events
- Hydrological modeling confirmed the effectiveness of GI on flood mitigation
- Cost-effectiveness of GI scenarios analyzed based on LCCA and hydrological indices
- Reasonable GI strategies proposed for flood mitigation in an urbanized watershed

GRAPHICAL ABSTRACT

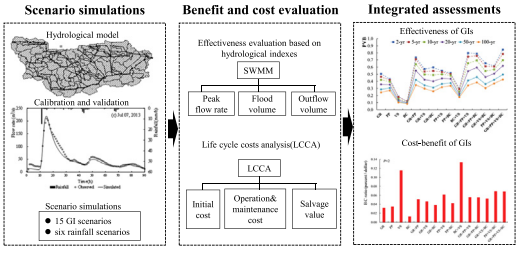

ARTICLE INFO

Article history:
Received 26 December 2017
Received in revised form 16 May 2018
Accepted 16 May 2018
Available online 26 May 2018

Editor: Zhen (Jason) He

Keywords:
Urban flood
Storm water management model
Life cycle cost analysis
Cost-effectiveness
Low impact development
Urbanization

ABSTRACT

Green Infrastructure (GI) has become increasingly important in urban stormwater management because of the effects of climate change and urbanization. To mitigate severe urban water-related problems, China is implementing GI at the national scale under its Sponge City Program (SCP). The SCP is currently in a pilot period, however, little attention has been paid to the cost-effectiveness of GI implementation in China. In this study, an evaluation framework based on the Storm Water Management Model (SWMM) and life cycle cost analysis (LCCA) was applied to undertake integrated assessments of the development of GI for flood mitigation, to support robust decision making regarding sponge city construction in urbanized watersheds. A baseline scenario and 15 GI scenarios under six design rainfall events with recurrence intervals ranging from 2–100 years were simulated and assessed. Model simulation results confirmed the effectiveness of GI for flood mitigation. Nevertheless, even under the most beneficial scenario, the results showed the hydrological performance of GI was incapable of eliminating flooding. Analysis indicated the bioretention cell (BC) plus vegetated swale (VS) scenario was the most cost-effective GI option for unit investment under all rainfall events. However, regarding the maximum potential of the implementation areas of all GI scenarios, the porous pavement plus BC + VS strategy was considered most reasonable for the study area. Although the optimal combinations are influenced by uncertainties in both the model and the GI parameters, the main trends and key insights derived remain unaffected; therefore, the conclusions are relevant regarding sponge city construction within the study area.

1. Introduction

Urban flooding has become one of the most frequent natural disasters in recent years (Buurman and Babovic, 2016; Wang et al., 2017). Urbanization converts natural land into urban infrastructure (e.g., buildings, parking lots, and roads) (Heilig, 2012), which is mostly

* Corresponding author at: No. 1 Yuyuantan South Road, Haidian District, 100038 Beijing, China.
E-mail addresses: meichao@iwhr.com, (C. Mei), liujh@iwhr.com, (J. Liu), wanghao@iwhr.com, (H. Wang), yangzy@iwhr.com, (Z. Yang), dingxy@iwhr.com, (X. Ding), shaoww@iwhr.com (W. Shao).

https://doi.org/10.1016/j.scitotenv.2018.05.199
0048-9697/

impervious and produces considerable hydrological effects (Jacobson, 2011; Liu et al., 2015a, 2015b). Of the various impacts, the most direct are the increases in flood frequency and volume, which intensify the risk, frequency, and extent of urban flood disasters (Chen et al., 2013; Pauleit et al., 2005). In the context of urban flood mitigation, traditional controls of urban stormwater mostly comprise gray infrastructure based on the strategy of removing runoff from a site as quickly as possible and then storing it at downstream facilities (Cembrano et al., 2004; USEPA, 2000). It is undeniable that gray infrastructure is necessary to deal with extreme rainstorms (Kamil et al., 2017); however, simply continuing to increase the capacity of gray infrastructure is considered unsustainable because of the pressures associated with ongoing climate change and urbanization (Hanak and Lund, 2012; Rosenberg et al., 2010). As an alternative to traditional gray infrastructure, green infrastructure (GI) has been used in many countries to mitigate urban flooding (Eckart et al., 2017; Kong et al., 2017). Previous studies have revealed that adoption of GI practices such as a green roof (GR), permeable pavement (PP), bioretention cell (BC), rain barrel (RB), and vegetated swale (VS) can be effective at reducing runoff, minimizing pollutant discharge, decreasing erosion, and maintaining the base flows of receiving streams. For example, Palla and Gnecco (2015) investigated the hydrological performance of GRs and PPs in a 5.5 ha urban catchment, and confirm the effectiveness of LID solutions even for the design storm event ($T = 2,5,10$ years); Liu et al. (2014) evaluated the effectiveness of different GI practices and their various combinations under different precipitation scenarios, results show that the reduction capacity for single GI facility was limited, especially in bigger storm events, and the integrated GI configuration has effective reduction percentage.

Recently, GI has been adopted as an important measure in many popular strategies of stormwater management, such as low impact development (LID), best management practice(BMP), and water sensitive urban design(WSUD) (Fletcher et al., 2016). In 2013, China proposed a new strategy for integrated urban water management named the Sponge City Program (SCP). The SCP deviates from the traditional rapid-draining approach (Wang et al., 2017). The new paradigm, which calls for natural systems such as soil and vegetation to be incorporated in urban runoff control strategies, is considered an ambitious national plan of GI implementation (Jia et al., 2017b). During 2015 and 2016, China selected 30 cities as pilot sites under the SCP. Each city is to receive 400–600 million RMB (1 RMB ~ 0.15 USD) annually from the central government for three years, with the total investment estimated to be about 42.3 billion RMB (Jiang et al., 2017). Currently, the investment and revenue mechanisms of the SCP are at an exploratory stage, and the cost-effectiveness of GI implementation has rarely been considered (Jia et al., 2017a). Following the three-year pilot period, robust decision making regarding sponge city construction will have to be based on integrated assessments of both the costs and the effectiveness of each SCP construction project. Many studies regarding sponge cities in China have evaluated the hydrological effects of GI implementation. For example, Hu et al. (2017) assessed the performances of LID practices in mitigating flood inundation hazards as retrofitting technologies in an urbanized watershed. Kong et al. (2017) explored the hydrological responses of stormwater runoff characteristics to four different land use conversion scenarios under multiple LID implementations. Previous studies have elucidated important information regarding GI implementation within the scope of the SCP in China.

These existing studies provide valuable revelations focusing on hydrological effects of and responses to GI implementation, or on cost-effectiveness analyses of single GI practices, at residential scale (Jia et al., 2014; Liu et al., 2014, 2015a, 2015b; Mao et al., 2017; Qin et al., 2013). Moreover, policymakers are currently faced with the increasingly difficult task of planning urban water management systems with regard to the uncertainties of climatic and socioeconomic changes (Babovic et al., 2017; Deng et al., 2013), which requires decision makers to plan storm water management infrastructure from economic standpoints and adaption pathways (Buurman and Babovic, 2016; Manocha and Babovic, 2017). For a specific area on the watershed scale, various GI options are possible within the scope of the SCP. However, the various GI practices have different hydrological impacts and costs; therefore, integrated assessments that include cost-effectiveness evaluations of potential GI selections in sponge city construction are indispensable (Liu et al., 2016; Xie et al., 2017). To support robust decision making regarding the selection of reasonable GI solutions for an urbanized watershed under the SCP, this study conducted integrated assessments of GI for flood mitigation and analyzed the cost-effectiveness of potential GI strategies.

This study adopted an integrated assessment framework that included hydrological performance evaluations and cost-effectiveness analyses based on the Storm Water Management Model (SWMM) (Brown, 1976) and life cycle cost analysis (LCCA) (Liao et al., 2014). The hydrological performances of different GI practices were investigated by comparison of scenario simulation results based on the SWMM. Then, flood mitigation performances versus life cycle costs (LCCs) were examined to evaluate the cost-effectiveness of different GI scenarios. Reasonable GI strategies that could potentially be implemented within the study area were identified based on integrated assessments that considered cost-effectiveness analyses and the actual situation. Indices for benefit evaluation and LCCA of GI implementation comprised key elements of the integrated assessment framework used in this study. A review of the literature revealed that reduction rates of runoff, peak flow, flood volume, and hydrograph delay are the indices used most frequently for benefit evaluation of GI implementation (Eckart et al., 2017; Palla and Gnecco, 2015; Xing et al., 2016). However, some studies have evaluated the performance and potential of GI in both mitigating flood inundation hazards and restoring the predevelopment water budget (Feng et al., 2016). The basic principles of applying the LCCA approach to GI practices appear clear and consistent. However, differences exist in the specific methods of cost calculation, and the question of whether to include land costs, salvage values, and the potential service period of the GI practices appears as the primary difference between the various LCCA approaches adopted. For example, Chui et al. (2016) evaluated the capital costs and the operation and maintenance costs (O&MC) of GI practices over an assumed lifespan of 30 years. Wang et al. (2016) estimated the cost of materials and construction and the O&MC for bioretention systems based on quantity calculations and an assumption that life cycle costs are related linearly to quantity. Liao et al. (2014) and Xie et al. (2017) performed LCCAs of GI practices with consideration of salvage value calculations and the different potential service periods of different GI practices. Overall, the selection of appropriate indices for benefit evaluation and LCCA depends on data availability, local standards, and personal preferences.

The primary purpose of this study was to conduct an integrated assessment of various GI options for flood mitigation in an urbanized watershed in China to support robust decision making for sponge city construction. The detailed objectives were (i) to quantify the effectiveness of potential GI options for flood mitigation under different rainfall scenarios, and (ii) to identify reasonable GI strategies that could be implemented within the study area.

2. Materials and methods

The integrated assessments of GI for flood mitigation were conducted based on an approach using the SWMM and LCCA, as shown by the schematic in Fig. 1.

2.1. Study area and data

2.1.1. Study area

The study area comprised the Liangshuihe (LSH) watershed, which is located in the south of downtown Beijing, China (39°41′24″–39°54′11″N, 116°14′44″–116°42′37″E) (Fig. 2). The district is a highly

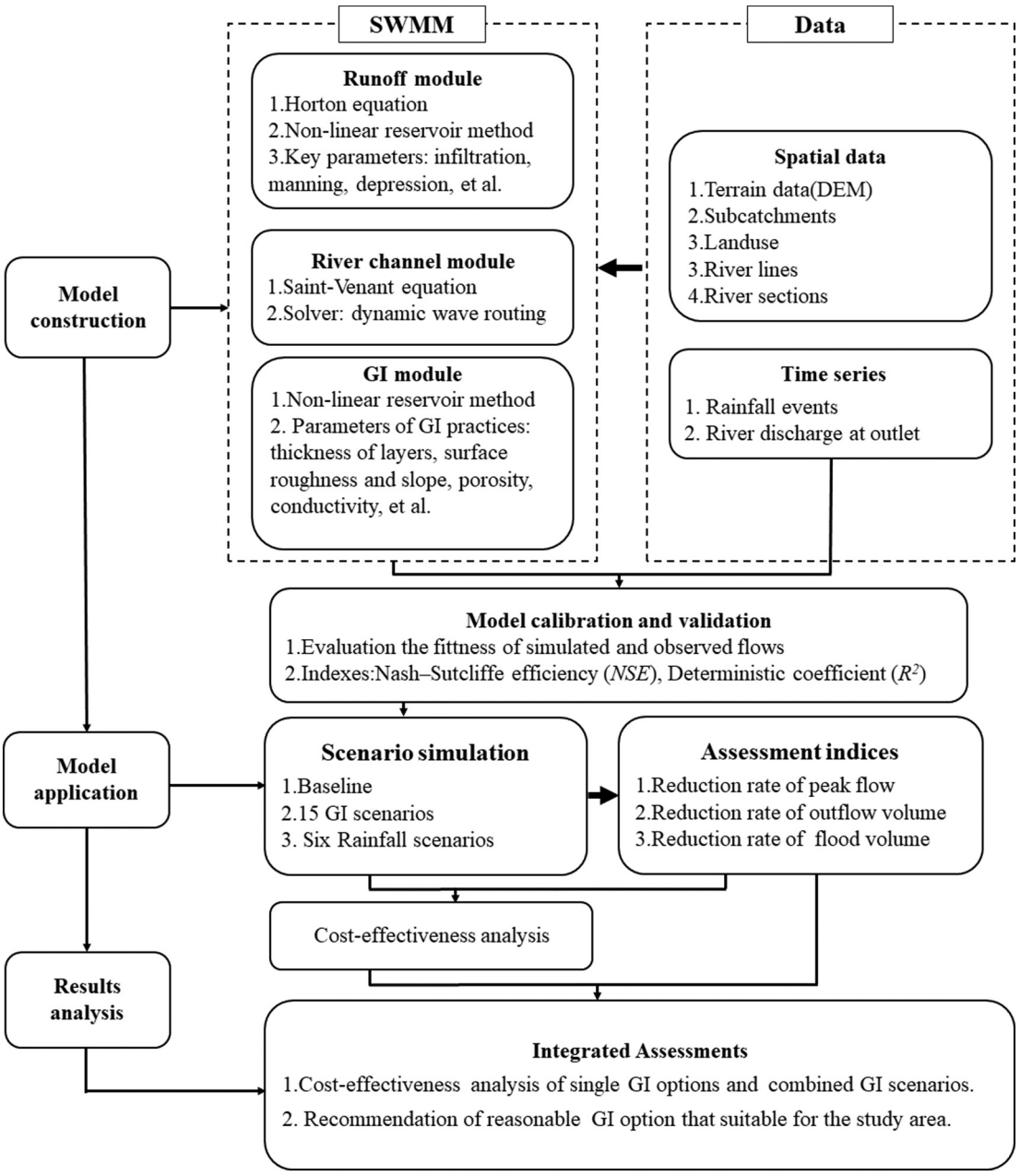

Fig. 1. Overall research framework of the study.

urbanized watershed covering an area of about 651.80 km^2. The LSH watershed is located in a region with a temperate monsoon climate that has four distinct seasons. The average annual rainfall is 522.4 mm, 81.6% of which falls during May–September. Over the past 30 years, the LSH watershed has experienced rapid urbanization, which has led to considerable increases in both population and building density. The high proportion of impervious surfaces, coupled with extreme rainfall in summer, can result in severe urban flood disasters in the LSH watershed, which have caused serious economic consequences and even loss of life in recent years. For instance, in the "7·21" flood disaster event in 2012, 36.5% of the flooded area was located in the LSH watershed. The SCP provides opportunities for mitigating urban flooding in the LSH watershed via the implementation of GI on the watershed scale. Therefore, the selection of reasonable GI strategies for implementation in the LSH watershed is important for robust decision making within the context of sponge city construction in China.

2.1.2. Data collection

The data used in this study were mainly provided by the Beijing Municipal Institute of City Planning & Design (BMICP&D, http://www.bjghy.com.cn/Default.aspx) and the Beijing Water Authority (BWA, http://www.bjwater.gov.cn/). Hydraulic parameters of the drainage system in the LSH watershed were collated from a flood prevention plan provided by the BWA, and land use data were collected from an urban development plan for Beijing provided by the BMICP&D. The spatial distribution and proportions of land use types within the study area are shown in Fig. 3 and Table 1, respectively. The terrain database comprised a 30 × 30 m DEM extracted from the freely available ASTER GDEM V2 (Fig. 1), which was developed by the Japanese METI and NASA. The BWA also provided data of observed 5-min rainfall and 30-min outflow at the outlet of the LSH watershed. Spatial data used in this study were saved in the ArcGIS Geodatabase in the form of electronic layers and managed by the ArcGIS Catalog 10.2.

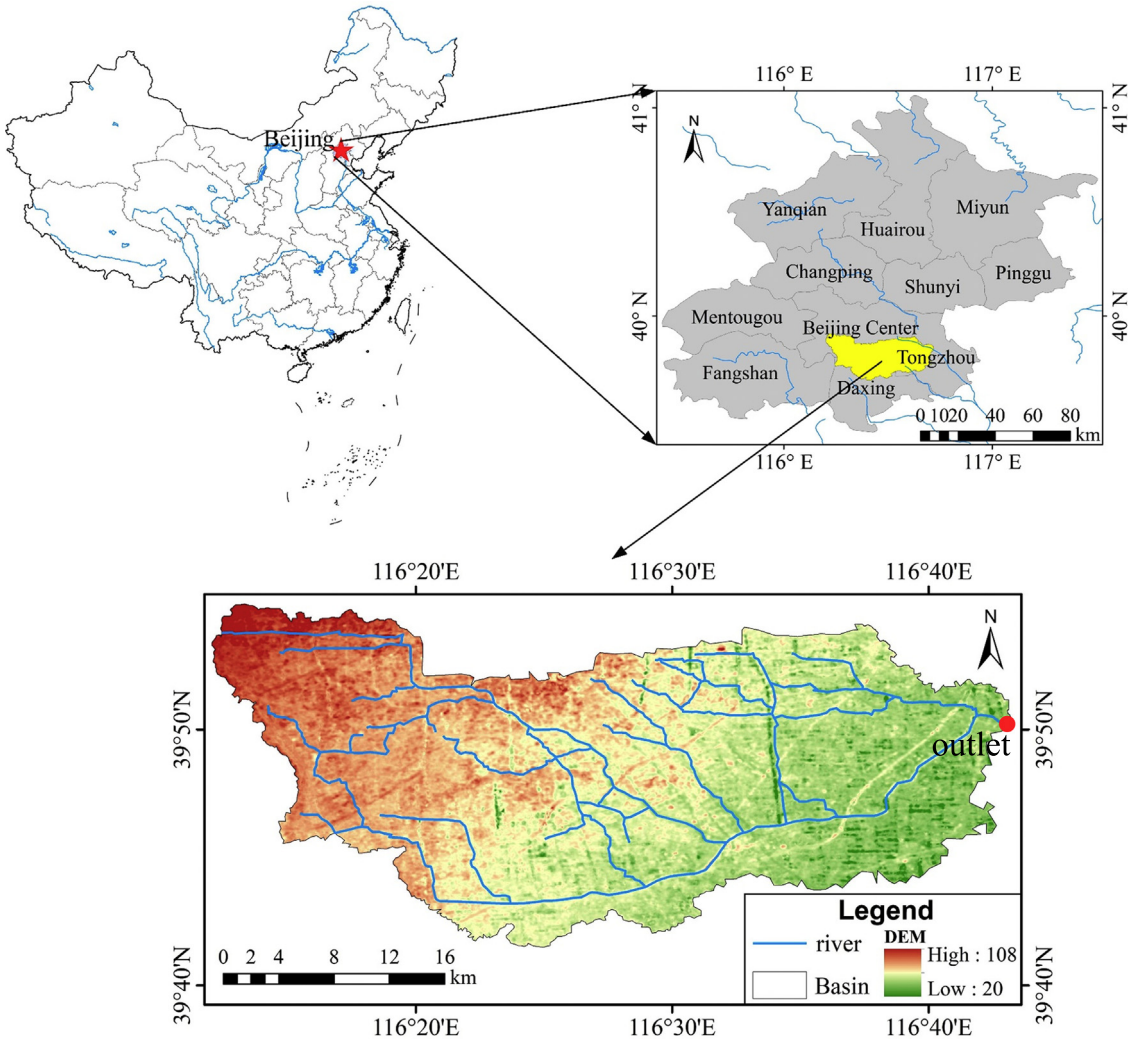

Fig. 2. Location and terrain of the study area.

2.2. Model setup

2.2.1. Hydrological model

The SWMM version 5.0.022, developed by the US EPA, was employed to simulate hydrological performances of the urban river system before and after GI implementation in the study area. The SWMM has been used widely for planning, analysis, and design related to stormwater in urban areas (Jia et al., 2014; Zhu et al., 2016). The SWMM version used in this study provides a LID control module, and it is one of the few models available with the capability to simulate the hydrological responses of GI practices. Hydrological performances of different types of GI practice such as GRs, PPs, BCs, and VSs can be modeled using the SWMM (Rossman, 2010). The GI practices in the SWMM are represented as combinations of vertical layers whose water balances and movements are computed during the simulation, and whose properties are defined on a per-unit-area basis (Chui et al., 2016) and assigned within selected sub-catchments in the model by defining corresponding areal coverages according to the GI scenario.

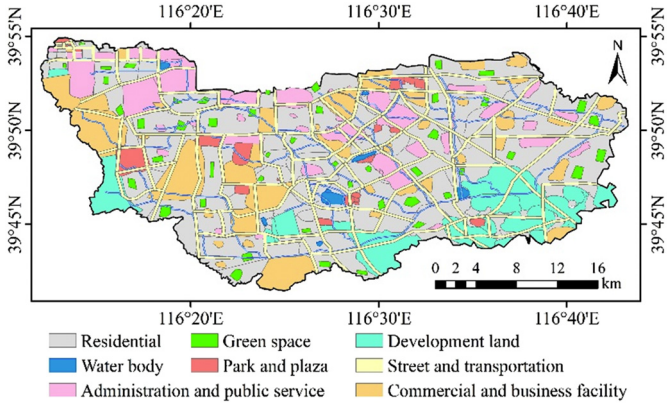

Fig. 3. Spatial distribution of land use within the study area.

Table 1
Land use characteristics of the LSH watershed.

Land use type	Total area (km^2)	Coverage (%)
Residential	197.50	30.30
Administration and public service	89.30	13.70
Commercial and business facility	121.23	18.60
Street and transportation	116.67	17.90
Park and plaza	16.30	2.50
Development land	69.09	10.60
Green space	24.77	3.80
Water body	16.95	2.60
Total	651.80	100.00

The SWMM provides alternatives for some typical hydrological processes. In this study, the Horton equation was used to estimate infiltration losses, and the representation of the rainfall-runoff process was based on the water balance approach and Manning's equation. Dynamic wave theory was used for the flow routing computation.

2.2.2. Model construction

The model for the LSH watershed was constructed with generalization of the real world, based on the detailed data and the principles of the SWMM construction. In addition, the following working assumptions were adopted: (1) rainfall intensity was the same throughout the entire study area; (2) daily dry weather sewage was set as an initial flow in the river systems; (3) all manholes were set at the turning points of the river channels and they were selected as nodes; and (4) runoff from each sub-catchment flowed into the nearest manhole.

To enable SWMM-based simulation of the LSH watershed, a set of physical components including sub-catchments, conduits, junctions, and outlets had to be developed first. The sub-catchment is a fundamental unit of a hydrological model. The sub-catchments used in the LSH model were defined based on the DEM and the road network because it is recognized that urbanization alters the surface hydrological characteristics; technical details regarding the use of the sub-catchment division method can be found in the literature (Kong et al., 2017; Shen and Zhang, 2015). The catchment division operation in this study produced a set of 78 sub-catchments for the LSH watershed (Fig. 4). The geometric properties of each sub-catchment (i.e., area, spatial coordinates, flow length and width, percentage of impervious surface cover, and slope) were subsequently quantified and added to the attribute table of the spatial dataset. Next, the drainage channels and river streams, together with flow directions within and between the sub-catchments and in situ observations, were used to generate detailed information on the characteristics of the conduits, junctions, and outlets. Consequently, 107 conduits, 98 junctions, and 1 outlet were defined (Fig. 4).

All the basic information was organized and analyzed using ArcGIS 10.2 and then converted to the *.inp* format of the SWMM; technical details regarding the use of the conversion method can be found in the literature (Kong et al., 2017).

In this study, the model calibration and validation strategy was based on comparison of the simulated and observed outflow hydrographs. Two universal indices were selected for evaluation: the Nash–Sutcliffe efficiency (*NSE*) index, which provides a quantitative assessment of the model accuracy in reproducing the outflow hydrographs (Nash and Sutcliffe, 1970), and the deterministic coefficient R^2 (Peng et al., 2015), which is used to assess the degree of correlation between the simulated and observed outflow time series. These indices were calculated according to Eqs. (1) and (2), respectively:

$$NSE = 1 - \frac{\sum_{t=1}^{n}\left(Q_t^{obs} - Q_t^{sim}\right)^2}{\sum_{t=1}^{n}\left(Q_t^{obs} - \overline{Q}_t^{obs}\right)^2}, \tag{1}$$

$$R^2 = \left(\frac{\sum_{t=1}^{n}\left(Q_t^{obs} - \overline{Q}_t^{obs}\right)\left(Q_t^{sim} - \overline{Q}_t^{sim}\right)}{\sqrt{\sum_{t=1}^{n}\left(Q_t^{obs} - \overline{Q}_t^{obs}\right)^2 \sum_{t=1}^{n}\left(Q_t^{sim} - \overline{Q}_t^{sim}\right)^2}}\right)^2. \tag{2}$$

2.3. Simulation scenarios of GI and storms

2.3.1. GI scenarios

In this study, the hypothetical numbers, types, and locations of GI were determined primarily based on the land use characteristics of the study area. Furthermore, "Technical Guide for Sponge Cities–Construction of Low-Impact Development" was referenced to determine the criteria for GI practice design (MHURD, 2014). In residential, administrative, and commercial areas, GI was designed mainly as GRs and PPs, whereas in areas of transportation, parks, plazas, and development land, PPs were the dominant GI implemented. Along the sides of roads, GI was set as VSs, whereas BCs were considered as appropriate GI in some areas of development land.

A summary of the GI practices considered for different land use types is shown in Table 2. The types and numbers of the hypothetical GI controls were specified on a per-unit-area basis according to the land use types of the study area. In this study, the building densities of different land use types were taken as their upper limits (Kong et al., 2017), according to the building density requirements in the detailed planning regulations of China. The areas of GI were allocated based on different land types and the specific characteristics of each sub-catchment. For example, the numbers and areas of GRs in residential zones were determined based on the building density and the potential coverage rate, and they were set for each sub-catchment in the developed SWMM. Specifically, the design parameters of GI practices were set in the model based on previous studies (Palla and Gnecco, 2015; Rossman, 2010), as presented in Appendix A.

Based on the methods for the setting of GI described above, 15 GI scenarios were proposed (for details, see Table 3), and the presented GI areas were taken as the maximum potential for the LSH watershed. The status quo scenario was defined as the baseline (BL), against which the effectiveness of each proposed GI scenario in terms of flood mitigation was quantified.

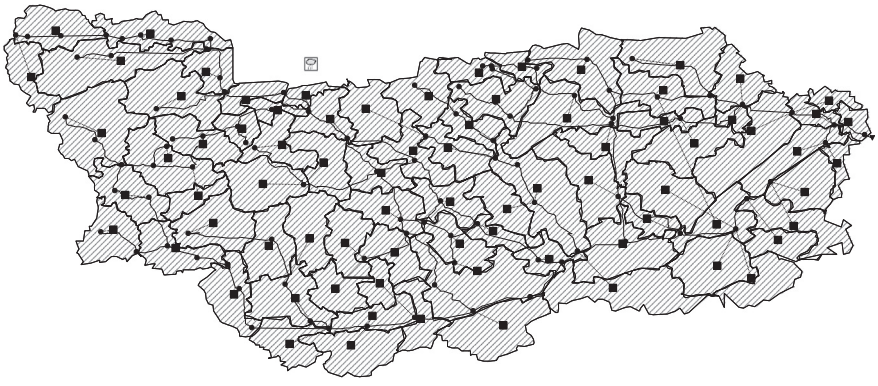

Fig. 4. Depiction of the LSH watershed used in the SWMM model with 78 sub-catchments and 107 conduits.

Table 2
Methods for setting GI practices for different land use types.

Land use type	GI Control	Set-up method
Residential	Green roof	Area × building density (0.35) × potential GR rate (0.50)
	Porous pavement	Area × [1 − greening rate (0.25) − building density (0.35)] × potential PP rate (0.50)
Administrative	Green roof	Area × building density (0.50) × potential GR rate (0.60)
	Porous pavement	Area × [1 − greening rate (0.25) − building density (0.50)] × potential PP rate (0.30)
Commercial	Green roof	Area × building density (0.60) × potential GR rate (0.80)
	Porous pavement	Area × [1 − greening rate (0.20) − building density (0.60)] × potential PP rate (0.50)
Transportation	Vegetated swale	Area × potential VS rate (0.20)
	Porous pavement	Area × potential PP rate (0.10)
Parks and plazas	Bioretention cell	Area × potential BC rate (0.20)
	Porous pavement	Area × potential PP rate (0.10)
Development	Vegetated swale	Area × potential VS rate (0.20)
	Porous pavement	Area × potential PP rate (0.10)

Note: "Area" in this table means the total coverage of the land use type of the study area. The potential coverage rates of GRs, PPs, BCs, and VSs refer to the maximum GI that could be implemented in each land use type. They were set according to the "Technical Guide for Sponge Cities–Construction of Low-Impact Development" (MHURD, 2014).

2.3.2. Design storm scenarios

In this study, synthetic hyetographs with six return periods (2, 5, 10, 20, 50, and 100 years) were used. The local storm intensity formula for Beijing is shown as Eq. (3) (Chang et al., 2016):

$$i = \frac{1602(1 + 1.037 \lg P)}{(t + 11.593)^{0.681}}, \quad (3)$$

where i is the storm intensity (mm/min), P is the design return period (year), and t is rainfall duration (min).

Hyetographs of the different design return periods were determined according to a rainfall pattern closest to the actual conditions using the Chicago Hydrograph Model (Keifer and Chu, 1957). Parameter r refers to the peak time point in the model, according to previous studies (Jia et al., 2014) and the local design manual, it ranges from 0–1. A reasonable range for r is 0.3–0.5; therefore, a value of 0.4 was chosen in this study. In addition, the rainfall duration was assumed as 120 min. The calculated synthetic hyetographs with 1-min time steps are shown in Fig. 5.

Table 3
Details of the 15 GI scenarios modeled in this study.

GI Scenario	Combination of GI practices and areas (km²)				Total area (km²)	Coverage (%)
	GR	PP	VS	BC		
GR	119.54				119.54	18.34
PP		78.53			78.53	12.05
VS			37.15		37.15	5.70
BC				3.26	3.26	0.50
GR + PP	119.54	78.53			198.07	30.39
GR + VS	119.54		37.15		156.69	24.04
GR + BC	119.54			3.26	122.8	18.84
PP + VS		78.53	37.15		115.68	17.75
PP + BC		78.53		3.26	81.79	12.55
BC + VS			37.15	3.26	40.41	6.20
GR + PP + VS	119.54	78.53	37.15		235.22	36.09
GR + PP + BC	119.54	78.53		3.26	201.33	30.89
GR + VS + BC	119.54		37.15	3.26	159.95	24.54
PP + VS + BC		78.53	37.15	3.26	118.94	18.25
GR + PP + VS + BC	119.54	78.53	37.15	3.26	238.48	36.59

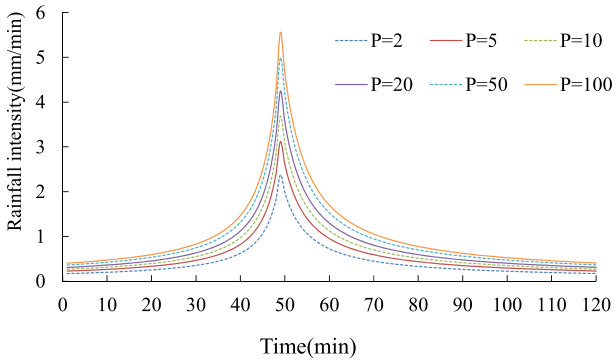

Fig. 5. Synthetic hyetographs of the six design rainfall scenarios in Beijing used in this study.

2.4. Integrated assessment method

2.4.1. Hydrological indices for flood mitigation assessments

The effectiveness of different GI scenarios can be evaluated with hydrological performance indices. Three indices were selected for this research in accordance with previous studies (Palla and Gnecco, 2015; Xing et al., 2016), i.e., the reduction rates of peak flow (R_p), outflow volume (R_o), and flood volume (R_f), which were calculated based on comparisons between the hydrological results of the GI scenarios and the BL. Here, peak flow refers to the highest flow rate of the runoff system, outflow volume refers to the total amount of discharge at the outlet, and flood volume represents the volume in excess of the channel capacity. The R_p index reflects the effects of GI implementation on the rainfall–runoff process, while the R_o and R_f indices represent the effectiveness of flood mitigation in river channels and overland, respectively. The three selected indices were considered to constitute a reasonably complete combination for the evaluation of the effectiveness of GI implementation. The values of peak flow, outflow volume, and flood volume were outputted by the SWMM in summary files of the simulations.

2.4.2. Cost-effectiveness analysis

Cost control is one of the primary concerns when promoting GI, especially on the watershed scale (Panagopoulos et al., 2011). In this study, the present value of benefit (PVB) and the present value of cost (PVC) were applied to analyze GI cost-effectiveness, represented here by the B/C value based on quantized values calculated using Eq. (4). The comprehensive B/C value can be used to illustrate the cost-effectiveness of specific GI practices or GI combinations. It has a strong relative attribute, where higher B/C values reflect greater cost-effectiveness of the GI implementation:

$$B/C = \frac{PVB}{PVC}, \quad (4)$$

where PVB is an index that reflects the flood mitigation benefit or effectiveness of the GI implementation, which can be calculated as:

$$PVB = (R_p + R_o + R_f)/3, \quad (5)$$

where R_p, R_o, and R_f are the reduction rates of peak flow, outflow volume, and flood volume, respectively, resulting from the implementation of different GI practices. For the reason that it is assumed that the three indices are important in the evaluation of urban flood reduction, PVB (unit: %) in this study was set as the arithmetic mean of the three indices adopted in this study.

The value of PVC in Eq. (4) was estimated using the LCCA method with consideration of all the costs associated with the project from the perspective of the system (Santos and Ferreira, 2013; Spatari et al., 2011). In accordance with the principles of the SCP, it was assumed that PPs, VSs, and BCs were incorporated in existing or mandatory infrastructure and that GRs did not occupy any land. Therefore, here, GI was assumed to incur zero land costs. The unit LCC of specific GI practices was then calculated using Eq. (6):

$$PVC_{x,n} = IC_x + \sum_{t=0}^{n} f_{r,t} \cdot O\&MC_t - f_{r,n} \cdot SV_n, \quad (6)$$

where $PVC_{x,n}$ is the *PVC* of GI practice *x* in year *n*, IC_x is the unit initial cost of GI practice *x* in the initial period of construction, $O\&MC_t$ is the annual cost of operation and maintenance in year *t*, SV_n is the salvage value (SV) of GI practice *x* in the end year *n* of the design life, $f_{r,t}$ is the present value factor of discount rate *r* in year *t*, and $f_{r,n}$ is the present value factor of discount rate *r* in the end year *n* of the design life. The unit of cost used in this study was the US dollar.

The SV of the GI practice was calculated using Eq. (7):

$$SV_n = \left(1 - \frac{i}{n}\right) O\&MC, \quad (7)$$

where *i* is the interval number from the last maintenance year to the design life year, which is assumed to equal 1 in this study in accordance with previous research (Liao et al., 2014).

The present value factors $f_{r,t}$ and $f_{r,n}$ were calculated using Eq. (8). Here, discount rate *r* was assumed as 5%, according to the latest monetary policy of the Chinese Central Bank (Liao et al., 2014):

$$f_{r,t} = \frac{1}{(1+r)^t}, \quad (8)$$

Because of the different area settings and various life cycles of different GI practices, comparison of the total *PVC* was unreasonable. Here, the *PVC* in Eq. (4) was represented by the unit annual average cost (*UAAC*) (Liao et al., 2014). The *UAAC*s of single GI practices and GI combinations were calculated using Eqs. (9) and (10), respectively:

For a single GI practice, $UAAC_x$ was calculated as:

$$UAAC_x = PVC_x / n_x, \quad (9)$$

For GI combinations, $UAAC_c$ was calculated as:

$$UAAC_c = \sum_{x=1}^{m} w_x \cdot UAAC_x. \quad (10)$$

In Eqs. (9) and (10), *x* refers to a specific GI practice, n_x is the design life of GI practice *x*, *m* is the number of different GI practices in a GI combination, and w_x is the areal proportion of each GI practice in the combination. Further details regarding the use of LCCA can be found elsewhere (Liao et al., 2014; Xie et al., 2017).

3. Results

3.1. Model calibration and validation

The LSH model was calibrated and validated against six rainfall–runoff events that occurred during 2011–2013. Specifically, three rainfall–runoff events (Jun 23, 2011, Sep 01, 2012, and Jul 07, 2013) were used for calibration and three events (Aug 26, 2011, Jul 21, 2012, and Jul 01, 2013) were used for validation. The model performances are summarized in Table 4 and illustrated in Fig. 6.

Fig. 6(a–c) shows the simulated hydrographs for the calibration events present acceptable representations of the complex measured outflows. In particular, the timings and the magnitudes of the peak flow rates are predicted reasonably well, as indicated by the *NSE* index and R^2 values of ≥0.83 and ≥0.85, respectively (Table 4). The results of the validation procedure reveal the suitability of the model for describing the hydrological responses of the urbanized watershed. The capability of the model in predicting the outflows is reflected in the *NSE* index and R^2 values of ≥0.75 and ≥0.85, respectively, for the three calibration events (Table 4). Fig. 6(d–f) shows that the model-simulated hydrographs satisfactorily reproduce the measured outflow regimes in terms of the timings and magnitudes of the peak flow rates. Thus, the calibration and validation results verified that the developed LSH model performs well in modeling the hydrological responses in the study area, and that it has potential for use in further scenario analyses. The best-fit model parameters are shown in Table 5.

Table 4
Model performance evaluation statistics.

Period	Events	Rainfall (mm)	NSE index	R^2
Calibration	Jun 23, 2011	68.9	0.96	0.85
	Sep 01, 2012	97.1	0.89	0.89
	Jul 07, 2013	98.5	0.83	0.97
Validation	Aug 26, 2011	68.2	0.88	0.96
	Jul 21, 2012	156.4	0.75	0.85
	Jul 01, 2013	60.8	0.92	0.89

3.2. Assessment of GI effectiveness in flood mitigation

Hydrological performances of the 15 GI scenarios implemented under the 6 rainfall events were investigated, and the hydrographs of the BL and GI scenarios are illustrated in Fig. 7. Hydrographs in Fig. 7 show peak flow reductions of varying magnitudes under the different GI scenarios, which reflect the altered hydrological regimes associated with GI implementation. It can be seen from Fig. 7a that the order of flood control effectiveness of single GI practices under the 2-year rainfall scenario is GR > PP > VS > BC, which is related both to the characteristics of the study area and to the properties of the specific GI practices. It is worth noting that the implementation of the combination of the four GI practices resulted in a reduction of peak flow of 80.62% and a 2-h hydrograph delay (Fig. 7a).

Reduction rates of the hydrological performance indices and PVB values for the 15 GI scenarios under the 6 rainfall events are shown in Fig. 8. The outflow volumes and flood volumes within the study area are obviously reduced by the GI implementations. Given that the three hydrological indices are related closely to flood risk, their distinct reduction implies mitigation of the urban flood hazard in the LSH watershed. The PVB is an integrated indicator that illustrates the benefit of the GI implementations, and the results presented in Fig. 8d confirm the effectiveness of GI on flood mitigation.

3.3. Integrated assessment of GI on flood mitigation

3.3.1. Cost analysis of single GI practices and GI combinations

The LCCs of single GI practices were calculated using the method described in Section 2.4.2. It is worth noting that the land costs of the various GI options were not considered when calculating the LCCs in this study. Table 6 presents the costs of each GI practice with reference to recent related research, together with generic intermediate values, which were used for the LCC calculations in this study. The unit LCCs of the GR, PP, VS, and BC GI practices were set as $317.10, $98.79, $31.72, and $186.90, respectively (Table 6). The VS practice is characterized by the lowest LCC, which can be attributed to the fact that this practice requires simple planning, design, and construction and minimal operation and maintenance. The UAACs of the 15 GI scenarios are presented in Fig. 9.

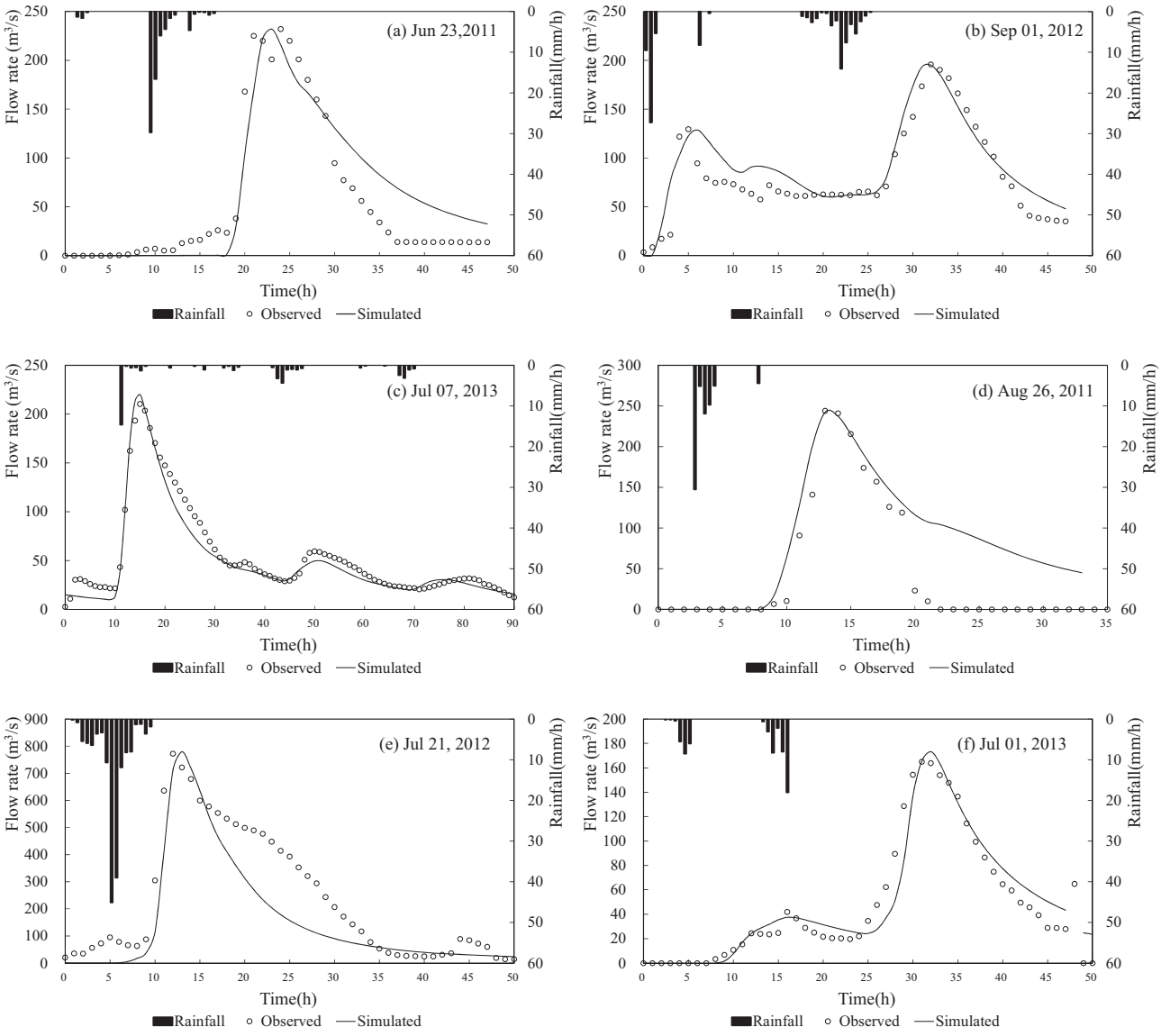

Fig. 6. Hyetographs, corresponding measured hydrographs, and comparisons of simulated hydrographs for the six rainfall–runoff events used for calibration and validation of the LSH model.

3.3.2. Cost-effectiveness assessments of different GI scenarios

Fig. 10 presents the B/C values of the different GI practices and GI combinations under the six rainfall events. For single GI practices (Fig. 10a), the B/C value decreases from 0.12 to 0.01 in the order: VS > PP > GR > BC and it decreases with increasing rainstorm return period. In terms of the B/C value, the order of the six combinations of two GI

Table 5
Best-fit model parameters of this study.

Parameters	Description	Value range[a]	Validated value[b,c,d,e]
N-imperv	Manning's roughness of impervious	0.001–0.1	0.04
N-perv	Manning's roughness of pervious	0.01–0.5	0.12
Dstore-imperv	Depression storage of impervious	0–5	1.62
Dstore-perv	Depression storage of pervious	3–10	7.83
MaxRate (mm/h)	Maximum infiltration capacity	10–200	85.72
MinRate (mm/h)	Minimum infiltration capacity	0–10	3.82
Decay constant (h)	Decay coefficient	2–7	6.70
Drying time (day)	Regeneration coefficient	2–14	7.00
N-river	Manning's roughness of rivers	0.01–0.10	0.027

[a] Rossman (2010).
[b] Chang et al. (2016).
[c] Zhao et al. (2016).
[d] Xie et al. (2017).
[e] Mei et al. (2017).

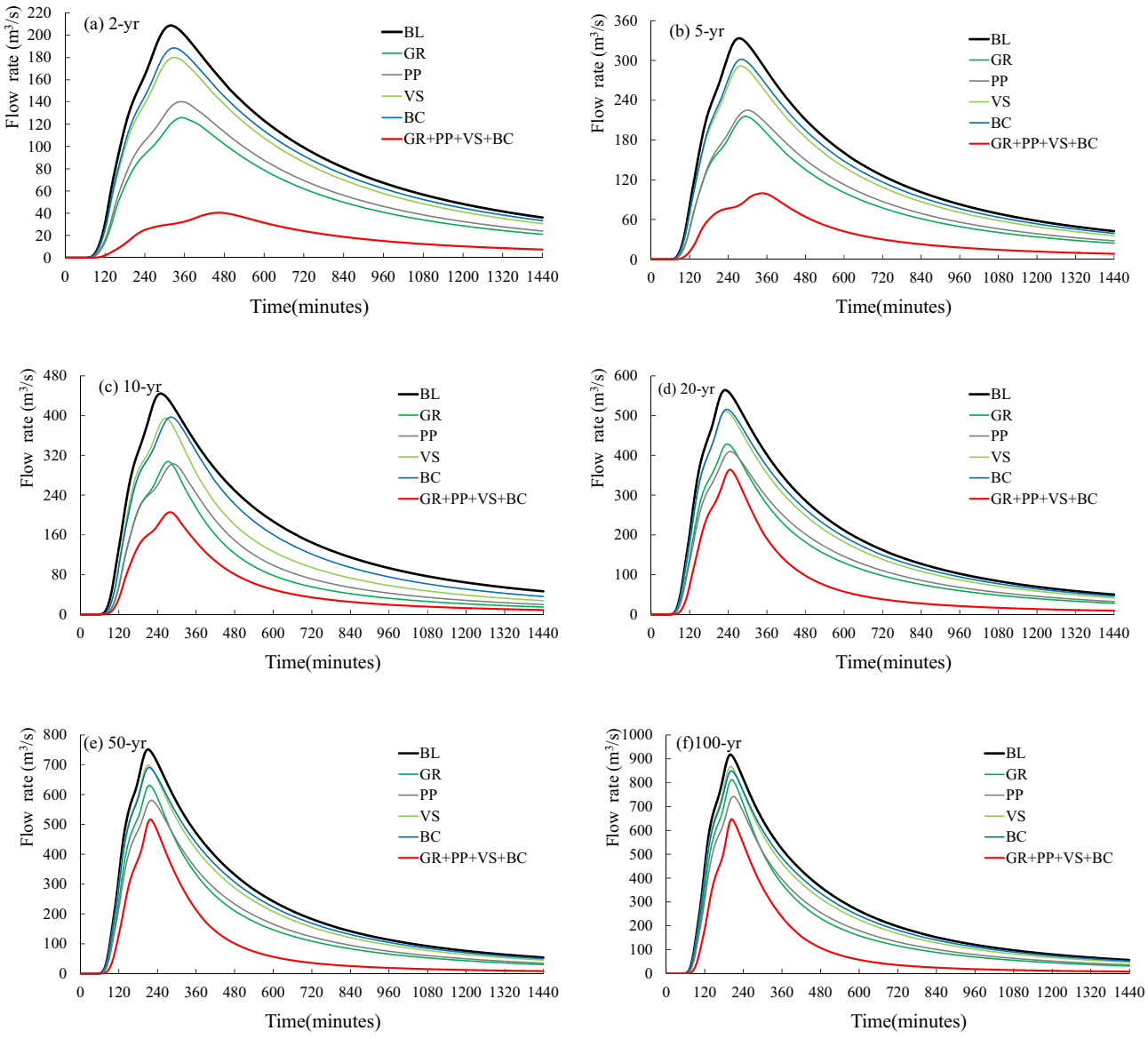

Fig. 7. Hydrographs of the BL and different GI scenarios under the six rainfall events.

practices is BC + VS > PP + VS > (PP + BC, GR + PP) > GR + VS > GR + BC (Fig. 10b), and the order of PP + BC and GR + PP changed depending on the rainfall return period. For the four combinations of three GI practices (Fig. 10c), the order in terms of the B/C value is PP + VS + BC > (GR + PP + VS, GR + PP + BC) > GR + VS + BC, and the B/C values range from 0.02 to 0.08%/dollar. The B/C value of the GR + PP + VS + BC practice has the same trend as the other combinations, i.e., it decreases with increasing rainfall return period from a value of 0.07 to 0.03%/dollar (Fig. 10d).

3.3.3. Integrated assessments of different GI scenarios

The B/C values of the different GI combinations are shown in Fig. 11, with return periods of rainfall events varying from 2–100 years. Given that the B/C value reflects the effectiveness of flood reduction per unit cost, the BC + VS combination is the most cost-effective GI option per unit investment under all six rainfall events in this study, followed by VS, PP + VS + BC, and GR + PP + VS + BC. However, the BC and VS areas implemented cover 3.26 (0.50%) and 37.15 (5.70%) km^2, respectively, of the study area. Therefore, to mitigate urban flooding effectively, combinations of three or four different GI practices with consideration of the practical situation would potentially be optimal for sponge city development of the LSH watershed.

Among the combinations of three or four GI practices, the PP + VS + BC practice is characterized by the lowest UAAC (Fig. 9) and the highest B/C value (Fig. 11), indicating that the implementation of this combination could obtain the highest benefit in terms of flood mitigation for the same investment cost. Therefore, the PP + VS + BC combination is recommended as the most reasonable GI option for the LSH watershed.

4. Discussion

4.1. Impacts of the explicit and implicit hypotheses

The SWMM was used for runoff simulations on the watershed scale, based on a series of explicit or implicit hypotheses; the implicit hypotheses have been described in this paper and some implicit assumptions are based on discipline consensus. The various assumptions of the modeling conditions, parameter specification, and data quality (Aich et al., 2016; Yu and Coulthard, 2015) could generate uncertainties. The uncertainties in relation to parameter specification and data resolution

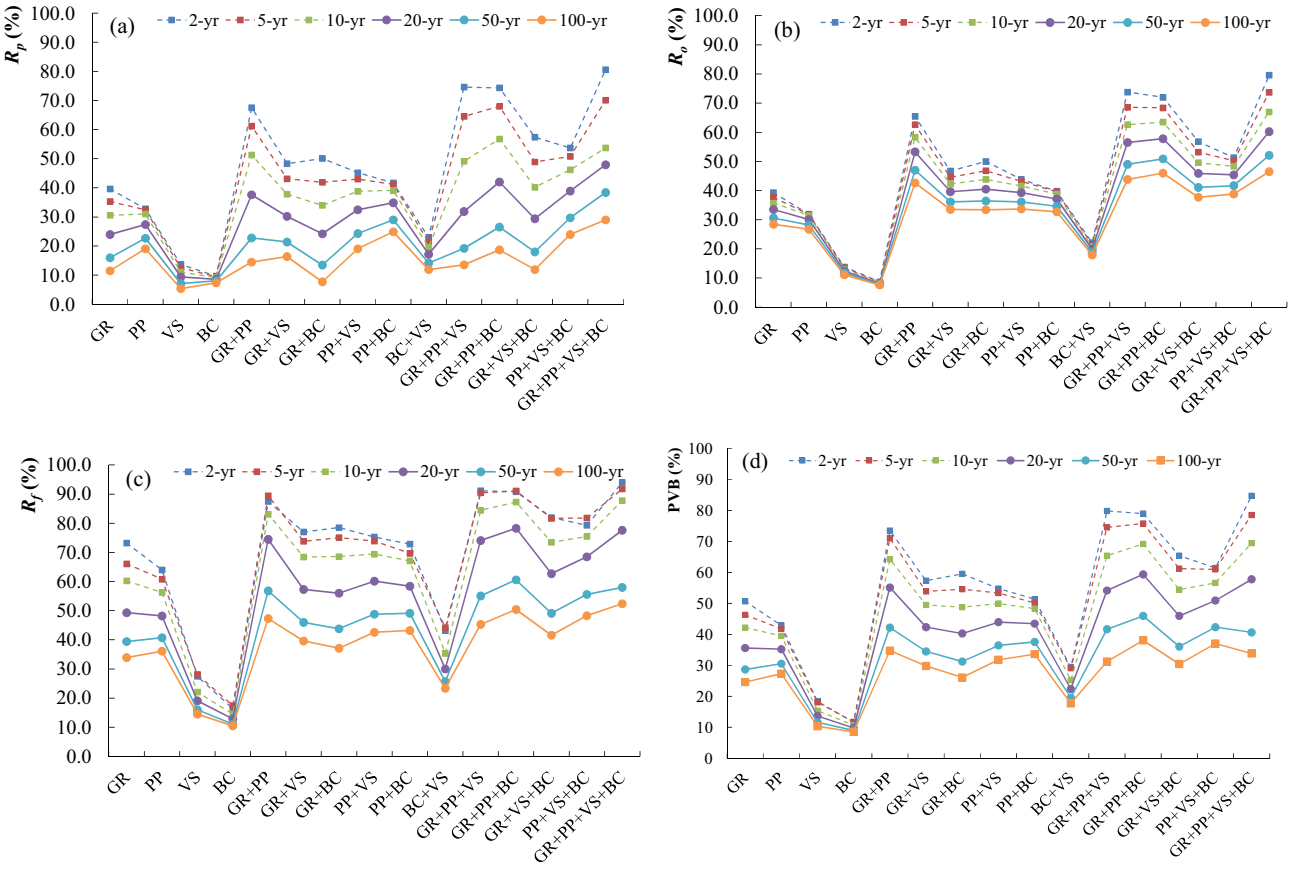

Fig. 8. Reduction rates of indices and PVB values for the 15 GI scenarios under the six rainfall events.

could introduce unavoidable errors in the derived results (Ozdemir and Dnm, 2013; Schubert et al., 2008); however, the deviation of the model output was considered acceptable and the model deemed satisfactory for scenario analysis. Thus, the uncertainties were considered not to affect the main trends and key insights derived, and the generic results are believed relevant to the design of reasonable strategies of GI implementation for the study area.

Limited events for the calibration of the hydrological model. The model parameters were adjusted using only six rainfall-runoff events. Thus, the model was calibrated based on a limited number of events and we extrapolated the model beyond the calibration runs to model 2–100-year events. Additional data will be used to improve and/or validate the model in future model simulations. However, the use of the current data allows us to conclude that the implementation of GI practices could be useful in limiting the consequences of storm events within the watershed.

The SWMM representation of GI practices at the watershed scale. First, the estimation of the potential areas of GI practices in this study could be considered optimistic, given that the methodology presented in Table 2 probably overestimates the real potential. It was assumed that all space belonging to the selected land use categories could effectively implement GI practices, meaning that the implementation of GI practices was technically possible. Second, different GI areas were considered unique entities at the sub-catchment scale without taking into account the spatial distribution of the specified land use and GI operations. Thus, we considered this representation suitable to assess the hydrological impacts of GI strategies at the watershed scale but not at the sub-catchment scale.

Table 6
Life cycle cost estimations of single GI practices.

GI	Unit initial cost			Unit O&MC		Unit salvage value		Life cycle cost (LCC)	Unit annual average cost (UAAC)
	Construction	Design and planning	Total cost	Percentages	Annual O&MC	Projected lifetime	Salvage value		
	Dollars/m^2	Dollars/m^2	Dollars/m^2	%	Dollars/m^2	Years	Dollars/m^2	Dollars	Dollars
GR	69–165[a]	–	69.00–165.00	6–16[d]	4.14–26.4	20[d]	14.51	317.10	15.86
PP	28–150[b]	3.36[c]	31.36–153.36	1[d]	0.28–1.50	8[g]	0.78	98.48	12.31
VS	26.25[c]	0.36[c]	26.61	1–2[e]	0.26–0.52	20[d]	0.37	31.72	1.59
BC	102.72[c]	3.39[c]	106.11	5–7[f]	5.14–7.19	20[d]	5.86	186.90	9.34

[a] Peck and Kuhn (2003).
[b] Xie et al. (2017).
[c] Liao et al. (2014).
[d] Liu et al. (2015a, 2015b).
[e] USEPA (1999).
[f] Weiss et al. (2005).
[g] Montalto et al. (2007).

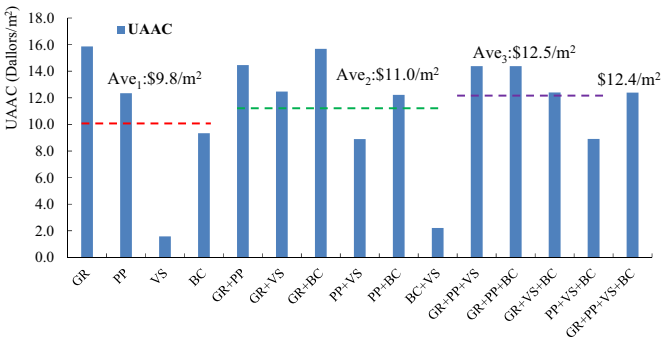

Fig. 9. UAACs of single GI practices and different GI combinations.

4.2. Flood mitigation of GI implementation

The results showed that GI is indeed effective in reducing flooding within the study area. For example, the peak flow reduction rate of the GR + PP + VS + BC scenario was as high as 80.62% under the 2-year rainfall scenario. However, flooding cannot be eliminated under the different GI scenarios for all rainfall events, and the effectiveness of the various GI practices was diminished under scenarios of heavier rainfall. Therefore, combinations of green and gray infrastructure will result in improved flood mitigation effects. Because of the high densities of buildings and population in urban areas, the implementation of GI often involves many stakeholders (Manocha and Babovic, 2017). However, the implementation of gray infrastructure reduces land occupation, indicating that combined development of green and gray infrastructure could be practical, even in megacities (Mell et al., 2016; Xie et al., 2017).

The GIs performance varies with the variations of rainfall scenarios, and the effectiveness decreased with the return period, that is because the GIs are infiltration-based flood control measures, and under heavy rainfall events the GIs are easier to saturate. In summary, this study confirms the effectiveness of GIs on flood mitigation.

4.3. Implications of cost-effectiveness analysis

The perspectives provided by the research results will benefit decision makers in relation to the adjustment of management strategies. For example, GRs are effective in flood mitigation because of their larger areal configuration and technical attributes; however, in comparison with other GI their costs are relatively high, which leads to lower B/C values for GI scenarios that include GRs. Clearly, GRs would be a better option if their maintenance costs were lower. Further analysis showed that O&MCs contribute the largest proportion of the LCCs for GRs; consequently, the reduction of O&MCs is important in relation to the implementation of GRs. In addition, the B/C values of GI combinations were shown to be higher than for single GI practices (except VSs), which suggests that GI combinations constitute more reasonable options than implementations of single GI practices.

The design parameters of GI practices have important impacts on flood mitigation effects, such as initial saturation, berm height, and hydraulic conductivity of the storage layers. Furthermore, the design parameters are also related to their LCCs; therefore, the effectiveness of GI with different design parameters should also be investigated under various rainfall scenarios. Previous studies have reported that different GI parameters show different sensitivities that are related to rainfall characteristics (Chui et al., 2016; Palla and Gnecco, 2015). This reinforces the necessity of undertaking GI simulation studies on various design parameters to support robust decision making in relation to sponge city construction. In the future, site-scale field experiments would be

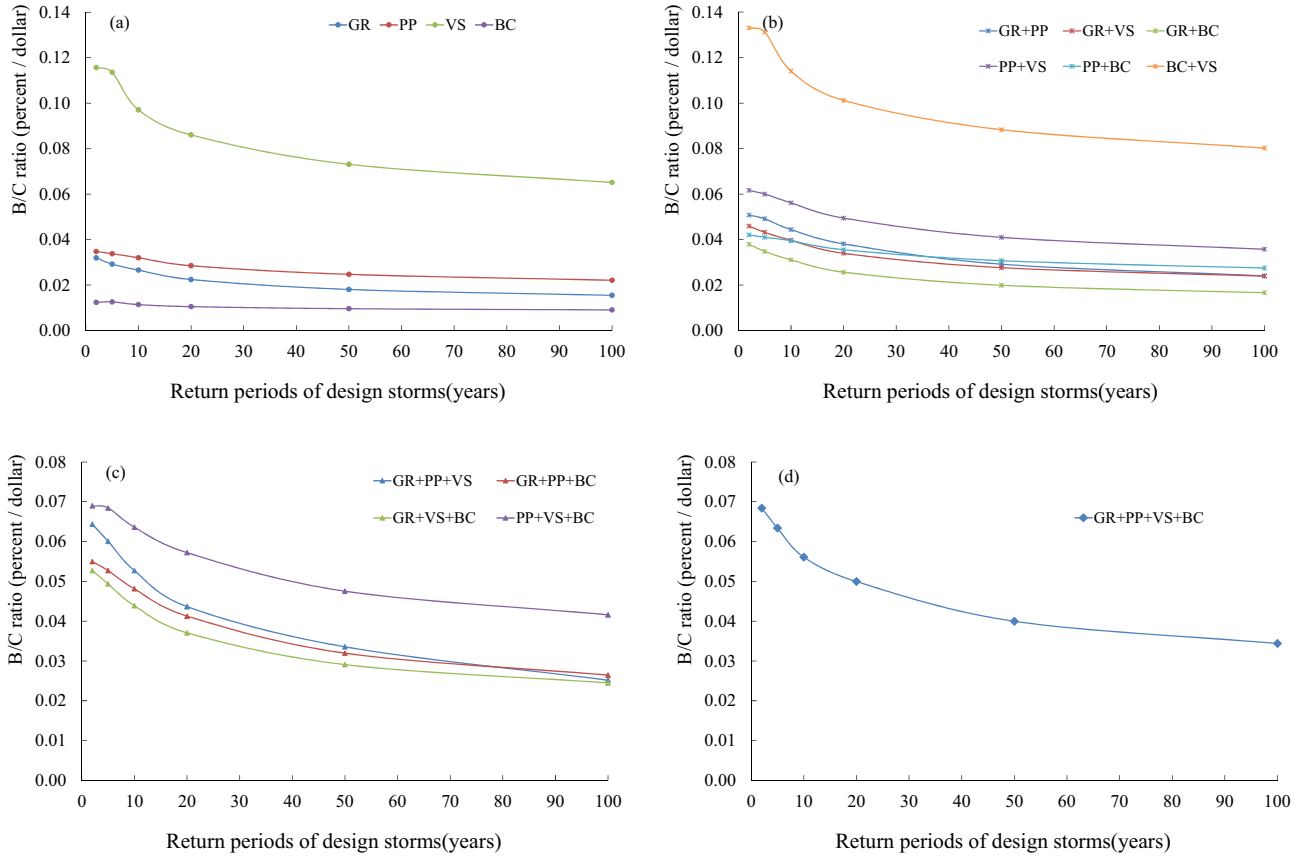

Fig. 10. Comparisons of the B/C values of the different GI scenarios under the six rainfall events.

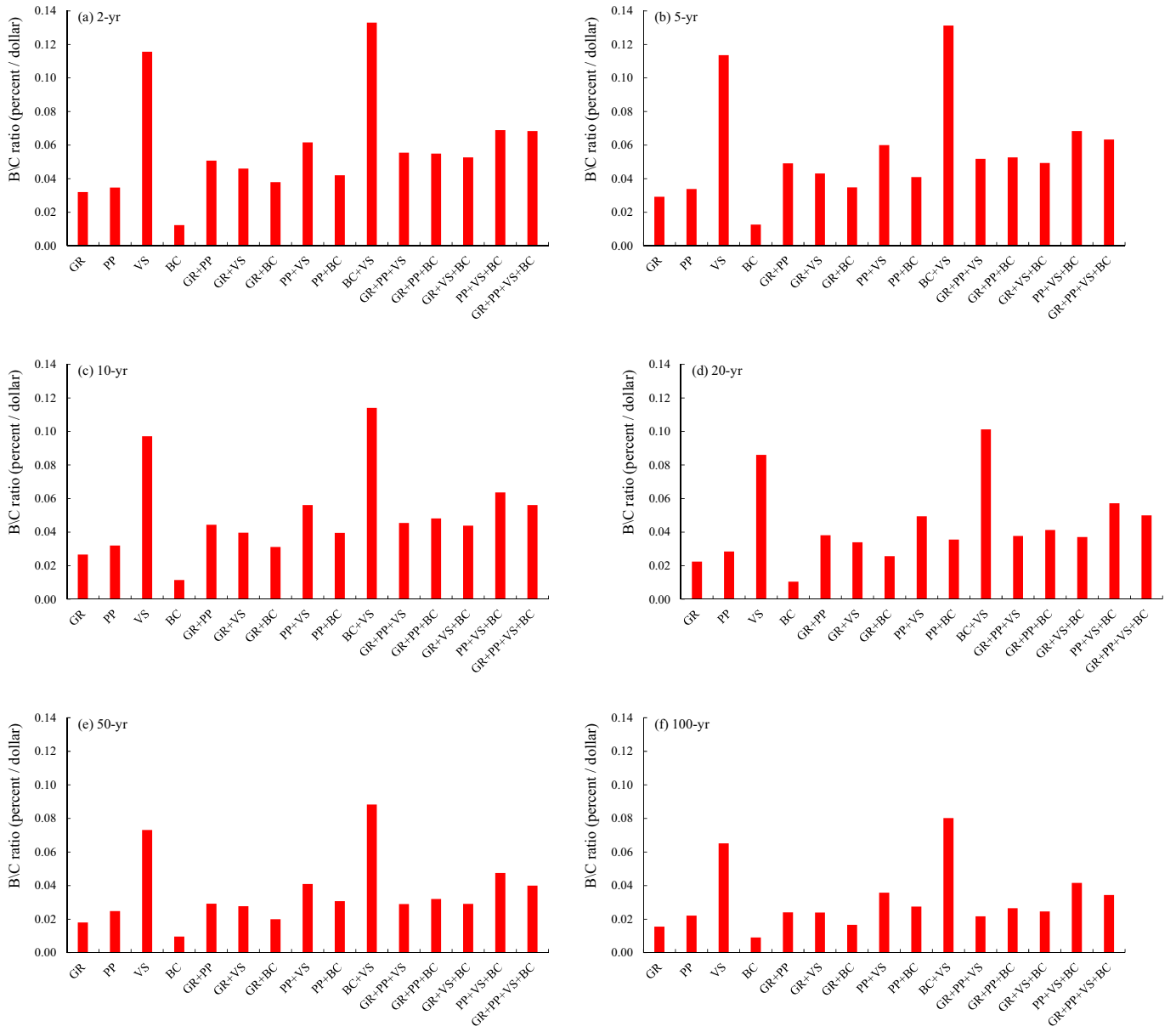

Fig. 11. Comparisons of B/C values of the 15 GI scenarios under the six rainfall events.

helpful in investigating reasonable GI design parameters in combination with water-scale scenario simulations.

It is worth noting the B/C orders and values are not absolute. In order to apply a more comprehensive indicator to represent the benefit, three indices were selected, and they hold equal weight in this study, however, it is an important point that related to the results, in further study, opinions form managers and various stakeholders should be considered for a more practical weight allocation of the indices for benefit evaluation. Greater attention should be given to both the main trends and key insights of the results and the reasonable GI options in the different areas (Liao et al., 2014; Xie et al., 2017). Simulation results are usually different from the actual situations because models are simply generalizations of the real world. Therefore, decision makers must consider the specific circumstances of the study area when making decisions regarding the promotion of sponge city construction in the LSH watershed.

4.4. Limitations of this study

There were some limitations to this study, and further study will needed in the future. First, there were some uncertainties relating to the calibration and validation of the model, and to the inputs and model structures. Second, the design parameters of the GI modeling lacked experimental data, and the effects of GI aging on the simulation results were not considered. For instance, PP performance will decrease obviously during its service lifetime because of clogging. However, the aim of this study was to determine reasonable strategies for the implementation of GI within the study area based on comparisons of the simulations. Consequently, these uncertainties and limitations will not have affected the derived conclusions.

5. Conclusions

To support robust decision making regarding sponge city construction in an urbanized watershed, this study performed an integrated assessment to identify potential cost-effective GI strategy that could mitigate urban flooding. The integrated evaluation framework based on the SWMM and LCCA was applied to the study area under six design storms with different return periods. The main conclusions are summarized as follows:

(1) The simulation results confirmed the effectiveness of GI implementation in the study area in mitigating urban flooding. However, the reduction rates of the flood-related hydrological indices decreased with increasing return periods of the design storms. Furthermore, no GI option was identified that could eliminate flooding. The findings indicated that GI should be combined with gray infrastructure to achieve optimal flood mitigation under extreme rainfall.
(2) The BC + VS combination was found the most cost-effective GI option for unit investment under all rainfall events. However, because of the limited area of possible implementation of the BC + VS strategy, combinations of three or four different GI practices were considered most suitable for the study area. Thus, the PP + BC + VS practice was recommended as the most reasonable GI option capable of providing the highest B/C value.

This study demonstrated the proposed integrated assessment technique could assist in the evaluation of GI strategies. The results highlight how detailed comparisons of various options are important and necessary in a robust decision-making process regarding sponge city construction, even though final decisions will be made with consideration of many local and practical conditions. Furthermore, a hydrological and LCCA model that is more detailed should be constructed in future study.

Acknowledgments

The authors would like to extend their thanks to both the National Natural Science Foundation of China (No. 51522907 & 51739011) and the National Key Research and Development Program of China (2016YFC0401401). This study was also supported by the Research Fund of the State Key Laboratory of Simulation and Regulation of Water Cycle in River Basin, China Institute of Water Resources and Hydropower Research (No. 2017ZY02). The authors would also like to extend their thanks to the three anonymous reviewers, this paper was totally improved according to their valuable comments and suggestions.

Conflicts of interest

The authors declare they have no conflicts of interest.

Appendix A. Design parameters for GI practices modeled in this study

Layers	Parameters	Units	GR	PP	VS	BC
Surface	Berm height	mm	50	20	250	50
	Vegetation volume fraction		0.8	0	0.8	0.8
	Surface roughness		0.24	0.015	0.03	–
	Surface slope	%	1	1	0.2	1
	Swale side slope	%	–	–	3	–
Soil	Thickness	mm	150	100	–	200
	Porosity		0.3	0.5	–	0.5
	Field capacity		0.2	0.2	–	0.2
	Wilting point		0.1	0.1	–	0.1
	Conductivity	mm/h	3.6	0.5	–	0.5
	Conductivity slope		10	10	–	10
	Suction head	mm	3.5	3.5	–	3.5
Storage	Thickness	mm	–	450	–	10
	Void ratio		–	0.63	–	0.75
	Seepage rate		–	3.3	–	0.5
	Clogging		–	0	–	–
Drain	Thickness	mm	100	–	–	–
	Void fraction		0.43	–	–	–
	Roughness		0.1	–	–	–
	Flow coefficient		–	0	–	–
	Flow exponent		–	0.5	–	–
	Offset height	mm	–	0	–	–
Pavement	Thickness	mm	–	100	–	–
	Void ratio		–	0.16	–	–
	Impervious surface	%	–	0	–	–
	Permeability	mm/h	–	254	–	–
	Clogging factor		–	0	–	–

References

Aich, V., Liersch, S., Vetter, T., Fournet, S., Andersson, J.C.M., Calmanti, S., Weert, F., Hattermann, F., Paton, E., 2016. Flood projections within the Niger River Basin under future land use and climate change. Sci.Total Environ. 562, 666–677.
Babovic, F., Babovic, V., Mijic, A., 2017. Antifragility and the development of urban water infrastructure. Int. J. Water Resour. Dev. 1–11.
Brown, LA., 1976. National symposium on urban hydrology and sediment control. July 27–29, 1976. Proceedings: National Symposium on Urban Hydrology, Hydraulics, and Sediment Control. ORES Publications, College of Engineering, University of Kentucky, p. 99.
Buurman, J., Babovic, V., 2016. Adaptation pathways and real options analysis: an approach to deep uncertainty in climate change adaptation policies. Policy Soc. 35 (2), 137–150.
Cembrano, G., Quevedo, J., Salamero, M., Puig, V., Figueras, J., Martı, J., 2004. Optimal control of urban drainage systems. A case study. Control. Eng. Pract. 12 (1), 1–9.
Chang, X., Xu, Z., Gang, Z., 2016. Urban rainfall-runoff simulations and assessment of low impact development facilities using SWMM model—a case study of Qinghe catchment in Beijing (in Chinese). J. Hydroelectric Eng. 35 (11), 84–93.
Chen, S.Y., Xue, Z.C., Li, M., Zhu, X., 2013. Variable sets method for urban flood vulnerability assessment. Sci. China Technol. Sci. 56 (12), 3129–3136.
Chui, T.F.M., Liu, X., Zhan, W., 2016. Assessing cost-effectiveness of specific lid practice designs in response to large storm events. J. Hydrol. 533, 353–364.
Deng, Y., Cardin, M.A., Babovic, V., Santhanakrishnan, D., Schmitter, P., Meshgi, A., 2013. Valuing flexibilities in the design of urban water management systems. Water Res. 47 (20), 7162–7174.
Eckart, K., Mcphee, Z., Bolisetti, T., 2017. Performance and implementation of low impact development-a review. Sci. Total Environ. 607–608, 413–432.
Feng, Y., Burian, S., Pomeroy, C., 2016. Potential of green infrastructure to restore predevelopment water budget of a semi-arid urban catchment. J. Hydrol. 542, 744–755.
Fletcher, T.D., Shuster, W., Hunt, W.F., Ashley, R., Butler, D., Arthur, S., et al., 2016. SUDS, LID, BMPs, WSUD and more – the evolution and application of terminology surrounding urban drainage. Urban Water J. 12 (7), 525–542.
Hanak, E., Lund, J.R., 2012. Adapting California's water management to climate change. Clim. Chang. 111 (1), 17–44.
Heilig, G.K., 2012. World Urbanization Prospects: The 2011 Revision. United Nations, Department of Economic and Social Affairs (DESA), Population Division-Population Estimates and Projections Section.
Hu, M., Sayama, T., Zhang, X., Tanaka, K., Takara, K., Yang, H., 2017. Evaluation of low impact development approach for mitigating flood inundation at a watershed scale in China. J. Environ. Manag. 193, 430–438.

Jacobson, C.R., 2011. Identification and quantification of the hydrological impacts of imperviousness in urban catchments: a review. J. Environ. Manag. 92 (6), 1438–1448.
Jia, H.F., Ma, H.T., Sun, Z.X., Yu, S., Ding, Y.W., Yun, L., 2014. A closed urban scenic river system using stormwater treated with lid-bmp technology in a revitalized historical district in China. Ecol. Eng. 71, 448–457.
Jia, H., Yu, S.L., Qin, H., 2017a. Low impact development and sponge city construction for urban stormwater management. Front. Environ. Sci. Eng. 11 (4), 20.
Jia, H.F., Zheng, W., Zhen, X.Y., 2017b. China's sponge city construction: a discussion on technical approaches. Front. Environ. Sci. Eng. 4, 39–49.
Jiang, Y., Zevenbergen, C., Fu, D., 2017. Understanding the challenges for the governance of China's "sponge cities" initiative to sustainably manage urban stormwater and flooding. Nat. Hazards 89 (1), 521–529.
Kamil, P., Daniel, S., Sabina, K., 2017. The temporal variability of a rainfall synthetic hyetograph for the dimensioning of stormwater retention tanks in small urban catchments. J. Hydrol. 549, 501–511.
Keifer, C.J., Chu, H.H., 1957. Synthetic storm pattern for drainage design. J. Hydraul. Div. 83 (4), 1–25.
Kong, F., Ban, Y., Yin, H., James, P., Dronova, I., 2017. Modeling stormwater management at the city district level in response to changes in land use and low impact development. Environ. Model Softw. 95, 132–142.
Liao, Z., Chen, H., Huang, F., Li, H., 2014. Cost-effectiveness analysis on LID measures of a highly urbanized area. Desalin. Water Treat. 56 (11), 2817–2823.
Liu, W., Chen, W., Peng, C., 2014. Assessing the effectiveness of green infrastructures on urban flooding reduction: a community scale study. Ecol. Model. 291 (1), 6–14.
Liu, Y., Ahiablame, L.M., Bralts, V.F., Engel, B.A., 2015a. Enhancing a rainfall-runoff model to assess the impacts of BMPs and LID practices on storm runoff. J. Environ. Manag. 147, 12–23.
Liu, Y., Bralts, V.F., Engel, B.A., 2015b. Evaluating the effectiveness of management practices on hydrology and water quality at watershed scale with a rainfallrunoff model. Sci. Total Environ. 511, 298–308.
Liu, Y., Theller, L.O., Pijanowski, B.C., Engel, B.A., 2016. Optimal selection and placement of green infrastructure to reduce impacts of land use change and climate change on hydrology and water quality: an application to the trail creek watershed, Indiana. Sci. Total Environ. 553, 149–163.
Manocha, N., Babovic, V., 2017. Development and valuation of adaptation pathways for storm water management infrastructure. Environ. Sci. Pol. 77, 86–97.
Mao, X., Jia, H., Yu, S.L., 2017. Assessing the ecological benefits of aggregate lid-BMPS through modelling. Ecol. Model. 353, 139–149.
Mei, C., Liu, J., Wang, H., 2017. Introduction of basic principle and application prospect for SWMM (in Chinese). Water Resour. Hydropower Eng. 48 (5), 33–42.
Mell, I.C., Henneberry, J., Hehl-Lange, S., Keskin, B., 2016. To green or not to green: establishing the economic value of green infrastructure investments in the wicker, Sheffield. Urban For. Urban Green. 18, 257–267.
MHURD, 2014. Ministry of housing and urban-rural development. Technical Guide for Sponge Cities-Construction of Low Impact Development (for Trial Implementation) http://www.mohurd.gov.cn/zcfg/jsbwj_0/jsbwjcsjs/201411/W020141102041225.pdf.
Montalto, F., Behr, C., Alfredo, K., Wolf, M., Arye, M., Walsh, M., 2007. Rapid assessment of the cost effectiveness of low impact development for CSO control. Landsc. Urban Plan. 82 (3), 117–131.
Nash, J.E., Sutcliffe, J.V., 1970. River flow forecasting through conceptual models, part I: a discussion of principles. J. Hydrol. 10, 282–290.
Ozdemir, I., Dnm, D., 2013. Modelling tree size diversity from airborne laser scanning using canopy height models with image texture measures. For. Ecol. Manag. 295 (5), 28–37.
Palla, A., Gnecco, I., 2015. Hydrologic modeling of low impact development systems at the urban catchment scale. J. Hydrol. 528, 361–368.
Panagopoulos, Y., Makropoulos, C., Mimikou, M., 2011. Reducing surface water pollution through the assessment of the cost effectiveness of BMPs at different spatial scales. J. Environ. Manag. 92 (10), 2823–2835.
Pauleit, S., Ennos, R., Yvonne Golding, Y., 2005. Modeling the environmental impacts of urban land use and land cover change-a study in Merseyside, UK. Landsc. Urban Plan. 71, 295–310.
Peck, S., Kuhn, M., 2003. Design Guidelines for Green Roofs, Ontario Association of Architects. CMHC, Ottawa.
Peng, H.Q., Liu, Y., Wang, H.W., Ma, L.M., 2015. Assessment of the service performance of drainage system and transformation of pipeline network based on urban combined sewer system model. Environ. Sci. Pollut. Res. Int. 22 (20), 15712–15721.
Qin, H.P., Li, Z.X., Fu, G., 2013. The effects of low impact development on urban flooding under different rainfall characteristics. J. Environ. Manag. 129 (18), 577–585.
Rosenberg, E.A., Keys, P.W., Booth, D.B., Hartley, D., Burkey, J., Steinemann, A.C., Lettenmaier, D.P., 2010. Precipitation extremes and the impacts of climate change on stormwater infrastructure in Washington State. Clim. Chang. 102 (1–2), 319–349.
Rossman, L.A., 2010. Storm Water Management Model User's Manual, Version 5.0. National Risk Management Research Laboratory, Office of Research and Development, US Environmental Protection Agency.
Santos, J., Ferreira, A., 2013. Life-cycle cost analysis system for pavement management at project level. Int. J. Pavement Eng. 14 (1), 71–84.
Schubert, J.E., Sanders, B.F., Smith, M.J., Wright, N.G., 2008. Unstructured mesh generation and landcover-based resistance for hydrodynamic modeling of urban flooding. Adv. Water Resour. 31 (12), 1603–1621.
Shen, J., Zhang, Q., 2015. A GIS-based sub-catchments division approach for SWMM. Open Civil Eng. J. 9 (1), 515–521.
Spatari, S., Yu, Z., Montalto, F.A., 2011. Life cycle implications of urban green infrastructure. Environ. Pollut. 159 (8–9), 2174–2179.
USEPA, 1999. Stormwater Technology Fact Sheet: Porous Pavement (EPA 832-F-99-023). https://www.epa.gov/owm/mtb/porouspa.pdf.
USEPA, 2000. Low Impact Development (LID): A Literature Review. United States Environmental Protection Agency. EPA-841-b-00e005. United States Environmental Protection Agency, Washington D.C.
Wang, M., Zhang, D., Adhityan, A., Ng, W.J., Dong, J., Tan, S.K., 2016. Assessing cost-effectiveness of bioretention on stormwater in response to climate change and urbanization for future scenarios. J. Hydrol. 543.
Wang, H., Mei, C., Liu, J.H., Shao, W.W., 2017. A new strategy for integrated urban water management in China: Sponge city. Sci. China Technol. Sci. 3, 317–329.
Weiss, P.T., Gulliver, J.S., Erickson, A.J., 2005. The Cost and Effectiveness of Stormwater Management Practices. Minnesota Department of Transportation Research Services Section, Minneapolis, MN.
Xie, J., Chen, H., Liao, Z., Gu, X., Zhu, D., Zhang, J., 2017. An integrated assessment of urban flooding mitigation strategies for robust decision making. Environ. Model. Softw. 95.
Xing, W., Li, P., Cao, S.B., Gan, L.L., Liu, F.L., Zuo, J.E., 2016. Layout effects and optimization of runoff storage and filtration facilities based on SWMM simulation in a demonstration area. Water Sci. Eng. 9 (2), 115–124.
Yu, D., Coulthard, T.J., 2015. Evaluating the importance of catchment hydrological parameters for urban surface water flood modelling using a simple hydro-inundation model. J Hydrol 524, 385–400.
Zhao, G., Shi, R., Pang, B., Xu, Z.X., Du, L.G., Chang, X.D., 2016. Impact of rapid urbanization on rainfall-runoff processes in urban catchment: case study for Liangshui river basin (in Chinese). J. Hydroelectric Eng. 35 (5), 55–64.
Zhu, Z., Chen, Z., Chen, X., He, P., 2016. Approach for evaluating inundation risks in urban drainage systems. Sci. Total Environ. 553, 1.